NURETH14-578

NUMERICAL ANALYSIS OF THERMAL STRATIFICATION IN THE REACTOR UPPER PLENUM OF MONJU WITH 1/3 SECTOR AND FULL SECTOR MODELS

M. SHIBAHARA, T. TAKATA and A. YAMAGUCHI

Osaka University, Suita, Osaka, Japan shibahara_m@qe.see.eng.osaka-u.ac.jp, takata_t@see.eng.osaka-u.ac.jp, yamaguchi@see.eng.osaka-u.ac.jp

Abstract

Three-dimensional analysis of thermal stratification phenomenon in the upper plenum of MONJU is conducted using FLUENT ver.12.1. This paper discusses the influence generated by upper core structure, which affects the flow structure near the core outlet region, and evaluates the thermal stratification phenomenon by the mean of comparing the full sector model built by the porous media approach with 1/3 sector model built by as-built geometry. Although there is a difference of the flow pattern from the core outlet between two models, the thermal stratification interface of 1/3 sector model shows the same trend with that of the full sector model.

1. Introduction

It is well known that the thermal stratification interface in the upper plenum is generated due to that the flow coasts down after the turbine trip. Since the temperature gradient near the thermal stratification interface would cause thermal stress in the reactor components, it is important to understand the characteristics of thermal stratification. In order to predict the temperature distribution after the turbine trip, many numerical analyses have been reported for various conditions. Ieda et al. [1] conducted the analysis of the thermal stratification for water and sodium with 1/10 scaled models using a multi-dimensional thermal hydraulic code, AQUA. In 1996, Doi et al. [2] performed the turbine trip test under the condition of 40% power operation. Moreover, they carried out the numerical analysis of the thermal stratification caused by the turbine trip using AQUA. Since it was complicated to model the Upper Core Structure (UCS) between Upper Internal Structure (UIS) and the core outlet, and flow holes on the inner barrel accurately, the pressure drop correlations were applied in the numerical analysis. In 2008, Yoshikawa et al. summarized the detailed engineering data of a test as a benchmark problem of the International Atomic Energy Agency (IAEA) [3]. Honda et al. [4] performed the numerical analysis of the upper plenum of Japan prototype FBR, MONJU, under the steady-state condition (40% power operation) using commercial code, FrontFlow/Red. In the numerical analysis, the UCS was reconstructed by mesh arrangement. The effect of buoyancy was also considered since the coolant temperature of the outer region of the core outlet (blanket subassembly) is lower than that of the inner core region. On the other hand, authors [5] have carried out the numerical simulation of the dynamic flow structure and thermal stratification phenomena of the upper plenum in MONJU using the

commercial code, FLUENT ver.12.1 [6]. In the numerical simulation of the full sector model, the UCS was assumed by a porous media approach. Then, the flow rate of flow hole was evaluated during the transient operation ranged from 0s (trip start) to 600s. As the result of numerical simulation, the flow structure changed from the steady-state condition as the flow rate and temperature of the core outlet decreased due to the turbine trip. Moreover, the interface of thermal stratification was influenced by the flow pattern in the upper plenum of MONJU. In this study, we discuss the influence generated by the UCS, which affects the flow structure near the core outlet region, and evaluates the thermal stratification phenomenon by the mean of comparing the full sector model built by the porous media approach with 1/3 sector model built by as-built geometry.

2. Analytical model

Figure 1 shows the analytical model in the numerical analysis. The full sector model of the upper plenum in MONJU is composed of Upper Internal Structure (UIS), TC-plug, core barrel, H/L pips (three loops), Fuel Handling Machine (FHM) and inner barrel with the flow holes. The fuel transfer machine lower guide and In-vessel racks are neglected for simplifying the full sector model. Moreover, since the UCS consists of complicated components such as Flow Guide Tubes (FGTs), Honeycomb Structure (HS), CR guide tubes and fingers, it is modelled using a porous media model with the porosity of 0.5 in the full sector model. Figure 2 illustrates the cross section of computational domain. In the present paper, two computational domains are calculated. The one is the above full sector model, and the other is 1/3 sector model which is a trisection of the full sector model including the H/L pipe (C-loop), as shown in Fig.2. The 1/3 sector model is represented by as-built geometry, where the geometry of the UCS includes the figures, the CR guide tubes, the HS and the FGTs.

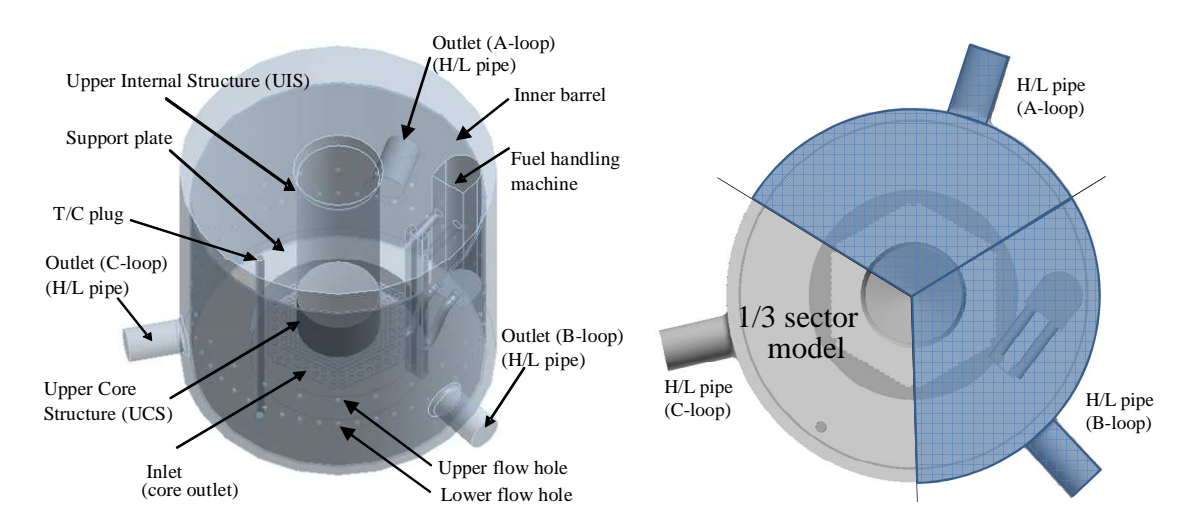
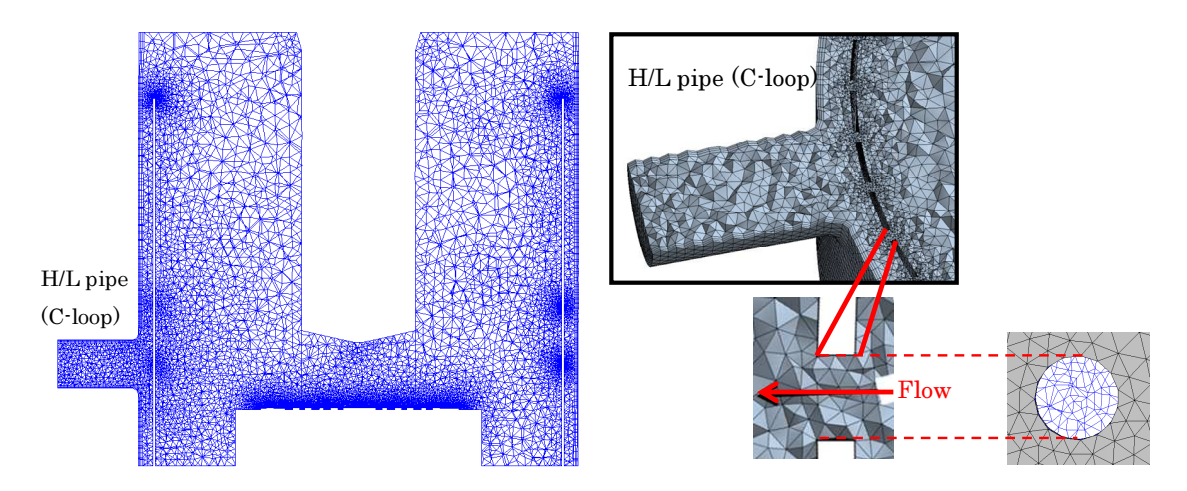


Figure 1 Analytical model

Figure 2 Computational domain

Figure 3 shows the mesh arrangement of (a) cross section of H/L pipe (C-loop) and (b) flow holes in the full sector model. The mesh numbers of full sector model are approximately 5.1 million. To analyse the flow distribution in the flow holes, the fine mesh in the flow holes is

arranged, as shown in Fig.3(b). Figure 4 shows the mesh arrangement of (a) cross section of H/L pipe (C-loop) and (b) the UCS in the 1/3 sector model. The mesh numbers of 1/3 sector model is approximately 11.4 million. The UCS is also reconstructed by mesh arrangement as shown in Fig.4(b). The flow rate and the sodium temperature at the inlet (core outlet) are based on the IAEA bench mark condition [3]. The reactor structures such as FHM, UIS, core barrel, support plate, H/L pipes, T/C plug, HS, CR guide tubes, fingers, FGTs and inner barrel are all adiabatic in this numerical solution. The outlet of H/L pipe is bounded with satisfying a constant pressure condition. In the lateral faces of the 1/3 sector model, symmetry boundary conditions are applied. Additionally, the physical properties of sodium are depended on the temperature [7]. Since the buoyancy force would be worked for the stratified flow, the effect of gravity is considered. In the analysis, the QUICK scheme is applied for convective terms so as to reduce numerical diffusion [8], and the time marching term is calculated by the second order Euler implicit method. Also, the SIMPLE method and the standard k-ε model are applied in FLUENT, ver.12.1.



(a) cross section of the full sector model (b) mesh arrangement of flow hole Figure 3 Mesh arrangement of the full sector model

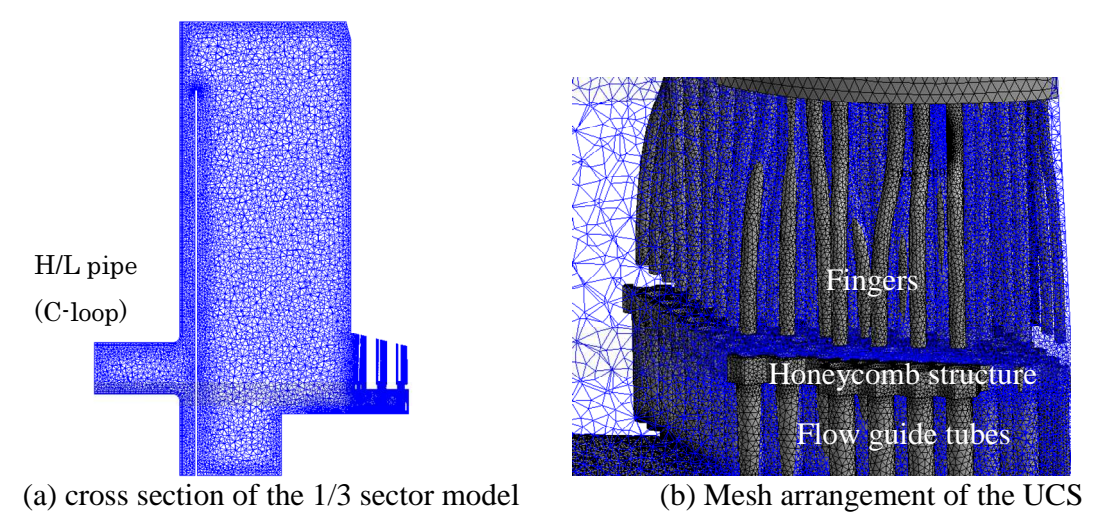


Figure 4 Mesh arrangement of the 1/3 sector model

3. Result and discussion

Figure 5 shows the typical flow patterns by comparing the 1/3 sector model on the left side with the full sector model on the right side ranged from 0s (trip start) to 1200s. Figure 5(a) illustrates the velocity profile at the trip start (0s). For the 1/3 sector model, a jet ascends from the core outlet through the HS, and impinges on UIS. The jet flows obliquely upward to the inner barrel and impinges the inner barrel, and then the flow branches off into two directions; upward flow and downward flow. The upward flow along the inner barrel overflows the top of the inner barrel, and then it descends through the annular gap between the inner barrel and the reactor vessel wall. The oblique flow from the core outlet to the inner barrel accounts for the main part in both models. And then, it can be seen from Fig.5(b) - (f) that the flow pattern has changed from the trip start condition due to the flow coasting down. As shown in Fig.5(b), the jet spreads to the upper plenum horizontally after it flows between the UIS and the core outlet. Then, the jet flows to the support plate. It is considered that the inertial force of jet becomes smaller than that of buoyancy effect. Due to the buoyancy, the hot sodium acts as the plug. After the coolant flow on the support plate, it flows to the lower flow holes. For the 1/3 sector model, the jet is divided into the upward flow through the HS and the transverse flow after impinging the HS. Since the fingers, the CR guide tubes, the FGTs, and the HS including flow holes of 36 and 32 mm dia. are represented explicitly, 1/3 sector model shows a different flow pathway compared with the full sector model. For the transient operation ranged from 240s to 600s shown in Fig.5 (c) - (e), the jet impinges the UIS since the total flow rate of the core outlet increases compared with that of 120s. Furthermore, the flow pattern has not changed since the plugging effect is greater than the inertial force. After 600s, as shown in Fig.5(f), the flow pattern has changed from the downward flow to the upward one since the temperature distribution of the lower region in the upper plenum becomes uniform. Thus, the inertial force of jet becomes bigger than the plugging effect due to the buoyancy.

Figure 6 shows the typical temperature profiles by comparing the 1/3 sector model on the left side with the full sector model on the right side ranged from 0s (trip start) to 1200s. As shown in Fig.6(a), the temperature profile indicates nonuniform at the trip start (0s). This is because the coolant temperature of the blanket subassembly is lower than that of the inner core region, so that the colder fluid descends along the core barrel and accumulates between the support plate and the lower flow holes. On the other hand, it can be seen from Fig.6(b)-(f) that the coolant penetrates the upper plenum since the core outlet temperature has reduced rapidly. The temperature variations result in density changes that affect the flow conditions. As shown in Fig.6(b), the thermal stratification interface is formed near the upper flow holes as the coolant is filled with lower part of the upper plenum. The buoyancy effect causes thermal stratification characterized by fluid distribution. After 120s, as shown in Fig.6(c)-(f), the interface of thermal stratification ascends due to bottom-up flow from the core outlet. In other words, the position of thermal stratification interface has been lifted with time. With the comparison between two models, it is understood that the temperature profiles of two models show the same trend, even if the flow pattern in the UCS is different between two models as shown in Fig.5. As a result, the thermal stratification interface of the upper plenum has a subtle influence of the flow pattern in the UCS.

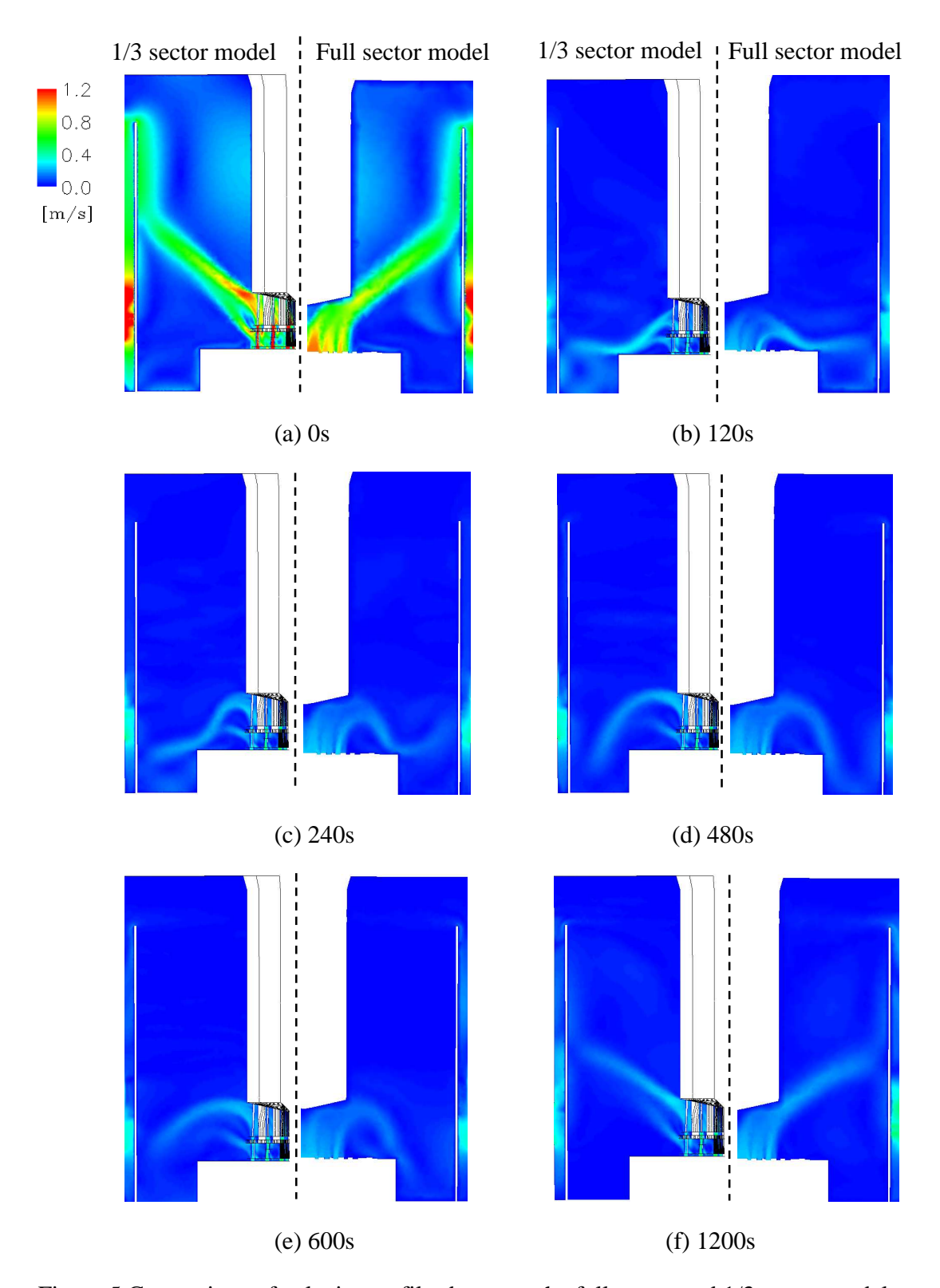


Figure 5 Comparison of velocity profiles between the full sector and 1/3 sector model ranged from the trip start (0s) to 1200s

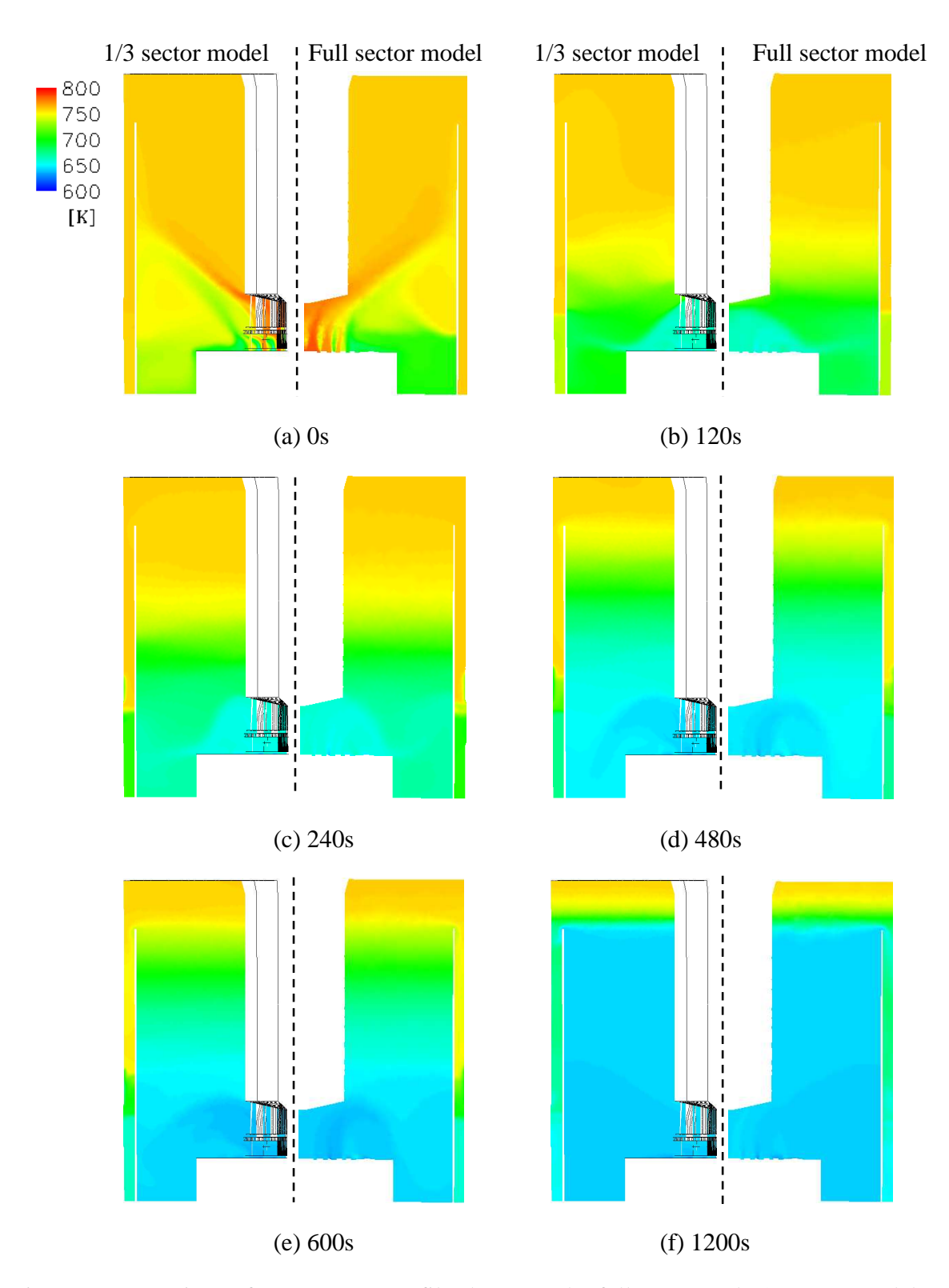


Figure 6 Comparison of temperature profiles between the full sector and 1/3 sector model ranged from the trip start (0s) to 1200s

Figure 7 shows the comparison of the axial temperature distributions between the analysis and the experimental data at the TC-plug [2]. The symbols show the experimental data after the turbine trip under the 40% power operation while the solid and dashed lines show numerical results of the full sector model and 1/3 sector model, respectively. As shown in Fig.7, the numerical results of two models show good agreement with the experimental data except for the depth lower than -6000 mm at the trip start (0s). It is considered that the thermocouple lower than -6000 mm is affected by the temperature of the support plate [4]. With the comparison between the numerical result of 1/3 sector model and that of full sector model, the numerical result of 1/3 sector model accords with that of the full sector model except for the steady-state condition. Figure 8 shows the velocity distribution under the steady-state condition for the 1/3 sector model on the left side and the full sector model on the right side. As shown in Fig. 8, it can be observed that flow structures of the lower region in the upper plenum are different between two models. Since the higher resolution mesh is used in the 1/3 sector model, the junction of the downward flow from the inner barrel and the vortex convection above the support plate is lower than that of the full sector model. The downward flow after impinging on the inner barrel is therefore mixed with colder coolant from neutron shielding and blanket subassemblies at the lower region of the upper plenum. Furthermore, it is also considered that the coolant of the neutron shielding and the blanket subassemblies are mixed with hotter transverse flow after impinging on the HS. Since liquid sodium has a high thermal conductivity, the temperature of the lower side of upper plenum in 1/3 sector model is higher than that of full sector model. With regard to the flow structure of the full sector model, a vortex flow generated by the neutron shielding and blanket subassembly also appears above the support plate in the upper plenum, however, the junction between downward flow from the inner barrel and the vortex convection above the support plate is higher than that of 1/3 sector model since the mesh arrangement of the full sector model is not finer than that of 1/3 sector model. Thus, the vortex at the lower region in the upper plenum is generated without mixing with the downward flow from the inner barrel, and the flow returns to the upper core barrel directly. Eventually, it is understood that the temperature at the lower region in the upper plenum becomes lower than that of 1/3 sector model. In the transient analysis, the temperature at the flow holes accords with the experimental data after the turbine trip, however, the lower temperature region swells rapidly both in the analyses rather than in the experiment after 240s. Thus, the temperature of the position higher than upper flow holes is underestimated. Figure 9 shows the elevation of the thermal stratification interface after the turbine trip. The solid and dashed lines show the numerical result of the full sector model and that of the 1/3 sector model, respectively. In order to evaluate the elevation of the thermal stratification interface, the non-dimensional temperature T* is defined as following equation;

$$T^* = \frac{T - T_c}{T_h - T_c} \tag{1}$$

where, T_c is minimum temperature, and T_h is maximum temperature. When the value of T^* become 0.5 both in the numerical analysis and the experiment, the position will be defined as the interface of thermal stratification. As shown in Fig.9, it is understood that the interface of the thermal stratification is raised as the coolant flows in the upper plenum. The trend of numerical values follows the experimental data at the early time ranged from the trip start (0s) to 240s. Thus, the rise of the interface in the experiment is suppressed comparing with that of numerical analysis during 240s-1200s. In other words, the plugging effect by the hot sodium is not weakening in the experiment during that period. With the comparison between the 1/3 sector and

the full sector model, the thermal stratification interface of 1/3 sector model shows the same trend with that of the full sector model in the numerical analysis, even though the flow pattern from the core outlet is different between two models as shown in Fig.5.

Figure 10 shows the (a) velocity and (b) temperature profiles at the horizontal cross section of (A-A') and (B-B') in the UCS at the trip start (0s). For the cross section of (A-A') and (B-B'), the upper region of the UCS and the HS are indicated in Fig.10, respectively. As shown in Fig.10(a), it seems that the jet impinged the UCS spreads through the fingers at the cross section of (A-A'). On the other hand, at the cross section of (B-B'), the jet from the flow guide tubes flows through the HS. Furthermore, the velocity distribution appears around the HS. This is because the jet without flowing the flow guide tube impinges on the HS, then it ascends around the HS. With regard to temperature profiles at the cross section of (A-A') and (B-B') as shown in Fig.10(b), it is considered that the temperature distributions in the UCS depend on the above flow profiles.

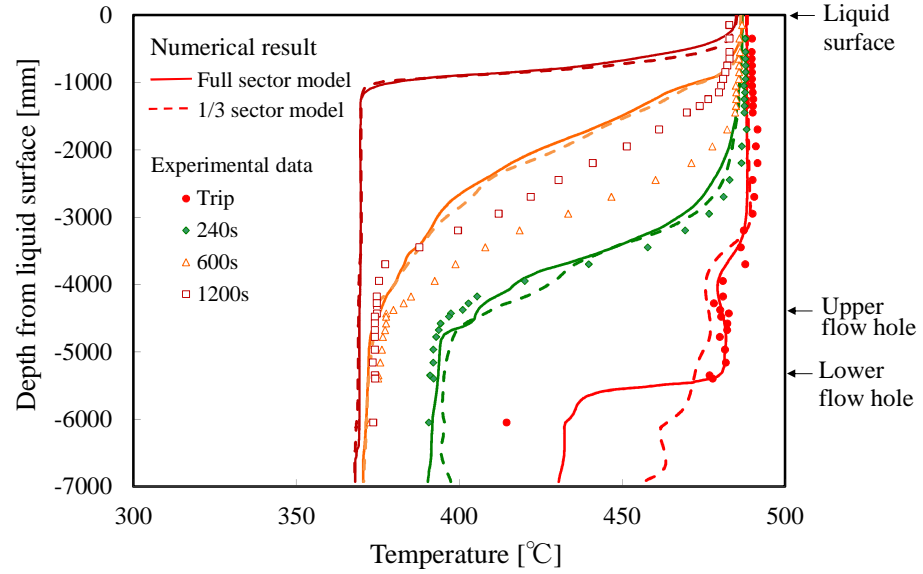


Figure 7 Temperature distributions ranged from the trip start (0s) to 1200s

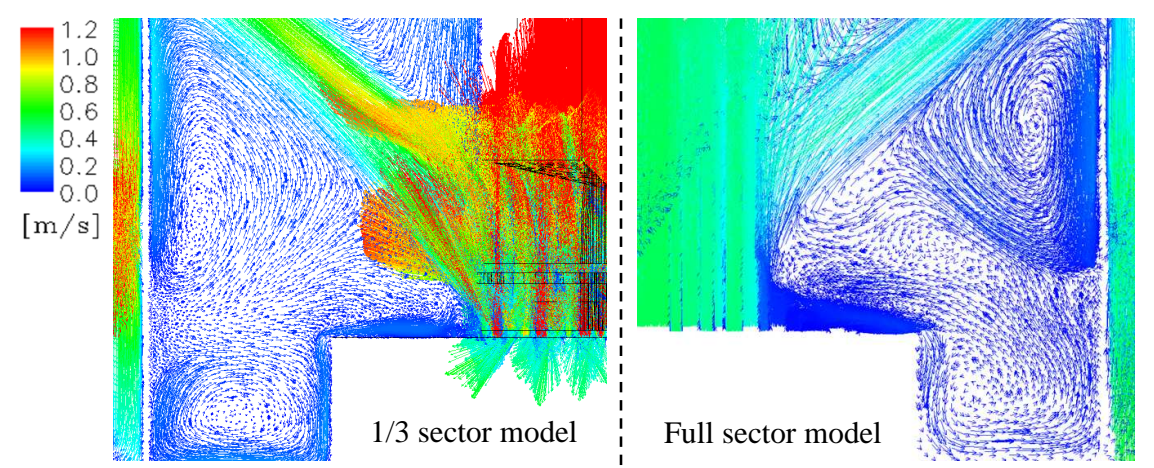


Figure 8 Velocity distributions under the steady-state condition

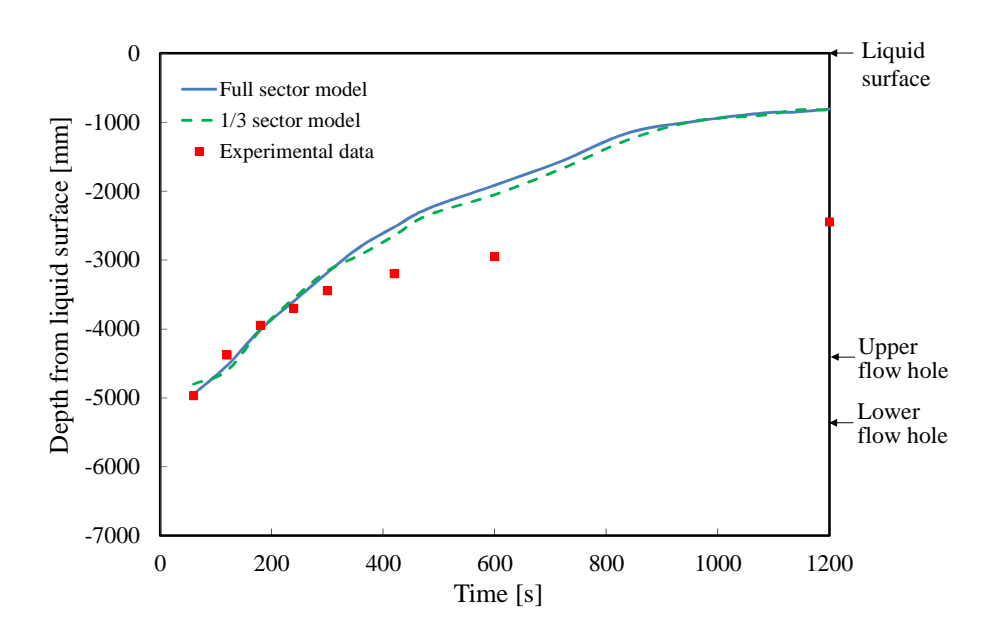


Figure 9 Elevation of thermal stratification interface after the turbine trip

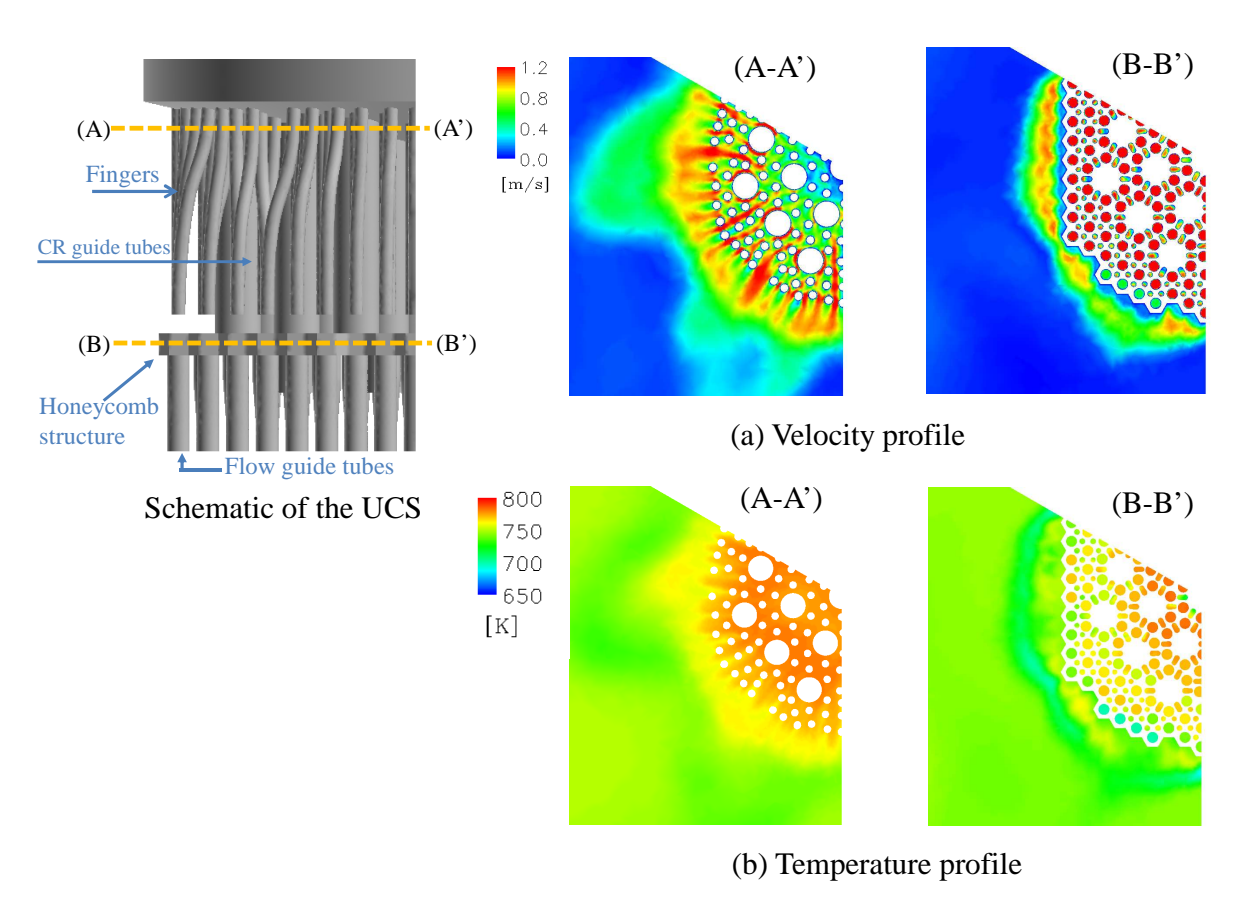


Figure 10 Velocity and temperature profiles in the UCS at the trip start (0s)

Figure 11 shows the (a) velocity and (b) temperature profiles at the cross section of (A-A'), and (B-B') at 240s. As shown in Fig.11(a), it is understood that the velocity in the UCS decreases comparing with that of the trip start (0s). On the other hand, as shown in Fig.11(b), it can be seen the uniform temperature distribution in the UCS. Also, almost no oscillation of the thermal stratification interface in the UCS is observed in the circumferential direction. It seems that the temperature in the UCS is mixed as the coolant flows through the HS and fingers after the turbine trip. At 240s after the turbine trip, the elevation of thermal stratification interface is higher than that of the UCS. In other words, the thermal stratification interface has already been lifted. Consequently, the temperature in the UCS becomes uniform at 240s although the coolant in the UCS flows through the HS and figures.

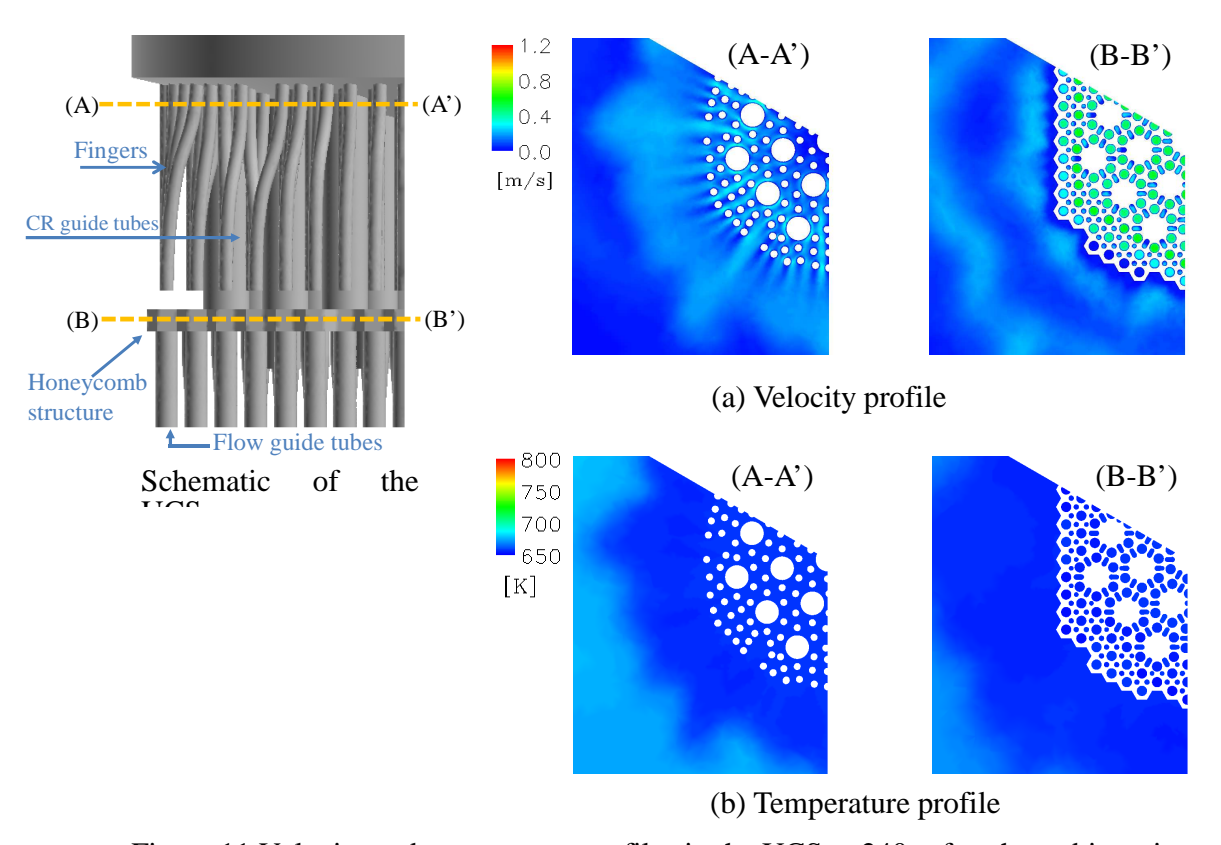


Figure 11 Velocity and temperature profiles in the UCS at 240s after the turbine trip

4. Conclusion

Three-dimensional analysis of thermal stratification phenomenon in the upper plenum of MONJU) was conducted using the commercial CFD code, FLUENT ver. 12.1. In this study, two computational domains were calculated. One was the full sector model in which internal structures (UIS, FHM, TC-plug, core barrel and inner barrel with flow holes) were directly modelled except the UCS. Because the UCS was complicated which includes CR guide tubes, flow guide tubes, HS and fingers, a porous media model was applied to simplify the full sector model. The other was the 1/3 sector model where the geometry of the UCS was also reconstructed by mesh arrangement. As the result, the flow pattern changed from obliquely flow beyond the top of inner barrel to downward flow through the flow holes. In other words,

the flow path of flow holes accounted for main part under the transient condition, since the hot sodium acted as the plug due to the buoyancy. Furthermore, the thermal stratification phenomenon was well simulated under the benchmark condition and compared with the experimental result until 240s from the trip start. After 240s, the thermal stratification interface was overestimated in these analyses. In addition, we discussed the influence of the UCS on the flow structure near the core outlet region and evaluated the thermal stratification phenomenon by the mean of comparing the full sector model by the porous media approach with 1/3 sector model by as-built geometry. Although there was a difference of the flow pattern from the core outlet between two models, the thermal stratification interface of 1/3 sector model showed the same trend with that of the full sector model.

5. Acknowledgment

Present study is the result of "2011 R&D core program for practical realization of fast breeder reactor by using MONJU" entrusted to "University of Fukui" by the Ministry of Education, Culture, Sports, Science and technology of Japan (MEXT).

6. References

- [1] Y. Ieda, I. Maekawa, T. Muramatsu, and S. Nakanishi, "Experimental and Analytical studies of the Thermal Stratification Phenomenon in the Outlet Plenum of Fast Breeder Reactor," Nuclear Engineering and Design, 120, 1990, pp.403-414.
- [2] Y. Doi, T. Muramatsu, and K. Kunoki, "Thermal Stratification Tests in MONJU Upper Plenum (I) Temperature Distribution under Normal and Scram Conditions with 40% Power Operation -," PNC TN9410 96-117, 1996. (in Japanese)
- [3] S. Yoshikawa, and M. Minami, "Data Description for Coordinated Research Project on Benchmark Analyses of Sodium Natural Convection in the Upper Plenum of the MONJU Reactor Vessel under Supervisory of Technical Working Group on Fast Reactors, International Atomic Energy Agency," JAEA-Data/Code 2008-024, 2008.
- [4] K. Honda, H. Ohira, M. Stotsu, and S. Yoshikawa, "Thermal-hydraulic Analysis of MONJU Upper Plenum under 40% Rated Power Operational Condition," <u>Proceedings of the 8th International Topical Meeting on Nuclear Thermal-Hydraulics, Operation and Safety (NUTHOS-8)</u>, Shanghai, China, 2010 October 10-14...
- [5] M. Shibahara, T. Takata, and A. Yamaguchi, "Numerical Simulation of Dynamic Flow Structure and Thermal Stratification Phenomena in LMFBR," <u>Proceedings of the 19th International Conference on Nuclear Engineering</u>, Chiba, Japan, 2011 May16-19.
- [6] ANSYS, Inc., "http://www.ansys.com/products/fluid-dynamics/fluent/".
- [7] Sodium Technology Handbook, JNC TN9410 2005-011, 2005. (in Japanese)
- [8] I.Maekawa, 1990, "Numerical Diffusion in Single-phase Multi-dimensional Thermal-hydraulic Analysis," Nucl., Eng. And Design, 120, pp.323-339.